EXPERIMENTAL AND NUMERICAL INVESTIGATIONS OF THE INTERACTION BETWEEN A PLASMA ARC AND A LASER

M. Schnick, S. Rose, U. Füssel, A. Mahrle, C. Demuth and E. Beyer

ABSTRACT

Plasma arc welding (PAW) is a modern welding technique for challenging joining tasks in a wide range of materials and plate thicknesses. A further improvement of the welding characteristics involving achievable welding speed, process stability and penetration depth is expected by an additional low energy laser beam with a maximum output power of 600 W. The paper presents an experimental and numerical analysis of the interaction between a plasma arc and a superimposed laser beam. The experiments are carried out with a non-concentric set-up of the plasma arc column and the laser beam. As results of bead-on-plate welding trials the cross-sectional weld areas were presented in order to demonstrate benefits of the combined process in comparison to separately conducted arc and laser welding. Furthermore, high speed video images (1 kHz frame rate) with synchronized current and voltage recording (1 MHz frame rate) were used. The experimental results demonstrate a different behaviour for welding steel and aluminium. In case of welding aluminium, an arc guidance was observed whereas destabilization effects occur for welding ferrous alloys. A numerical magneto hydro dynamical (MHD) arc model with a concentric set-up of arc column and laser beam set-up was aimed to improve our understanding of relevant interaction phenomena between the plasma arc and the laser beam.

IIW-Thesaurus keywords: Argon; Electric arcs; Lasers; Laser beams; Plasma; Plasma welding; Simulating.

1 Introduction

Plasma arc welding provides the productive and high performance joining of iron, titanium and aluminium. For an increase of the welding speed, the weld penetration and the stability of the process the plasma arc can be supported by laser radiation. In general, disadvantages of the single joining processes can be compensated by such a combined technique. However, the most of published scientific work concerning such hybrid joining technologies was aimed to high power laser processes of several kW and their advancement by welding arcs [1]. In these cases, the arc undertakes only an assisting function compensating some characteristic drawbacks of laser beam welding processes.

The combination of a welding arc with a low power ($P_L \leq 600$ W) laser provides the approach to influence mainly the arc column or the arc attachment by coupling the laser energy directly with the process region. Research results of Steen [2] or Cui and Decker [3-5] have already demonstrated that a laser beam of some hundred Watt to 2 kW is capable of stabilizing a TIG arc. They demonstrated an increased heat flux density due to a focussed arc attachment and a decreased arc voltage drop. Steen [2] traces back these effects to a locally increased number of free charge carriers at the anode surface. Otherwise, it was shown for a 0.2 mm-thick titanium sheet that an arc stabilization happened, even if the laser beam and the arc were positioned at the opposite sides of a workpiece. Cui and Decker [3-5] point out the influence of metal vapour, which results from the laser-induced evaporations of base material. They assume a local increase of the electric conductivity of the plasma. Albright *et al.* [6] demonstrate low power laser arc assistance due to a provided pre-ionisation of an arc root. Recent works of Hermsdorf *et al.* [7, 8] underline the role of the optogalvanic effect which is present in the arc column and, in particular, at the cathodic workpiece in gas metal arc welding (GMAW).

The present paper is focussed on investigations of a welding process with a combined heat source consisting of a plasma arc and a laser beam with a maximum output of 600 W. The work is aimed to characterize the interaction between the arc column and the laser beam and to comment the involved physical effects. In contrast to TIG arcs, which have been already investigated intensively, the plasma arc is characterized by significantly increased plasma flow velocities and energy densities in the arc column [9, 10]. Both provoke a high stability of the arc column. A fibre laser was used as the laser beam source, which permits a nearly diffraction-limited beam quality. This enables high energy densities at the workpiece. The interactions were studied for welding mild and stainless steels and aluminium alloys as well. The work is based on experimental investigations and numerical MHD-simulations.

Doc. IIW-2218, recommended for publication by Study Group SG-212 "The Physics of Welding."

2 Experimental set-up

The experiments were done using a non-concentric configuration of the plasma torch and the laser beam, which are both inclined with respect to the surface of the metal sheet being welded, see Figure 1. An Yb-fibre laser (IPG) was used with a laser wavelength of 1 070 nm and a minimum focus radius of 20 µm. The applied plasma arc system consists of a water-cooled plasma torch (ABIPLAS WELD 150) and a constant current power source (EWM Tetrix 400) using DC-EN-polarity. The parameters being constant during the experiments are the electric current of 100 A, the plasma gas flow rate of 0.8 l/min argon and the bore diameter of 2.6 mm in the plasma nozzle. Figure 1 shows the experimental set-up used.

A high-speed video camera with a resolution of 1k by 1k pixel and 1 000 frames per second (fps) was used for a visual process observation. Simultaneously, the synchronized values of the electric current and the arc voltage were recorded with sampling rate of 1 MHz. The camera was positioned perpendicular to the welding direction. Suitable narrow band pass filters were used in order to improve the observation of the arc root at the workpiece.

3 Experimental results

The interaction of the arc and the laser beam was investigated for bead-on-plate welding of aluminium alloys and steels. A significant influence of the laser on the arc behaviour was mainly observed for aluminium plates, Figure 2. Without laser beam action, two arc roots and attachments are established as a result of the inclined arrangement of the plasma torch. One arc root and attachment is on axis with the plasma torch (a). The second one is transient and specifies the arc root of the lowest electric resistance (b). It was observed that both arc roots compete to each other and thus no continuous welding seam was produced.

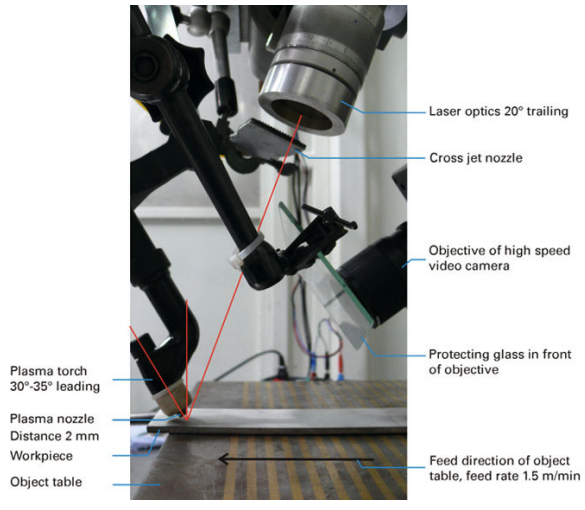

Figure 1 – Experimental set-up

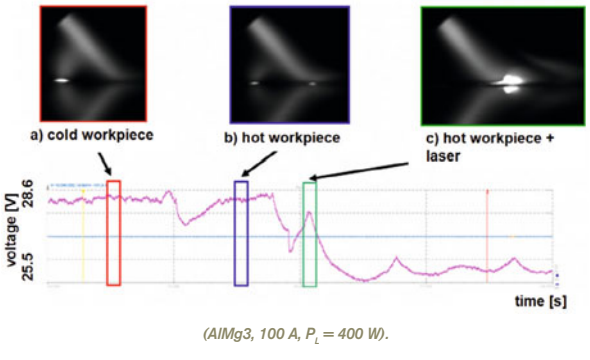

(AlMg3, 100 A, P_L = 400 W).

Figure 2 – Arc roots and the attachments [(a) and b) without laser and in the laser spot c)] and the characteristic arc voltage behaviour of a plasma arc with and without laser beam

However, after switching the laser on, the arc attachment is fixed at the laser-generated hot spot (c) and the arc column is stabilized.

The top of Figure 2 shows the ability to track the plasma arc attachment at an aluminium workpiece by a laser of 400 W. The involved interactions between the laser beam and the arc plasma decrease the arc voltage. The reduction is a nearly linear function of the applied laser power. It is about 3 V for a laser beam power of P_L = 600 W, see Figure 3.

Besides the arc root stabilization it was possible to move the arc attachment sidewards, forwards and backwards up to 2 mm, which is about half of the free arc length. Therefore the arc attachment at aluminium can be favourably controlled by a laser beam.

Figure 4 shows cross-sections in AlSi1MgMn sheets which were produced by plasma arc or laser only and by plasma arc and laser. The combination of both energy sources causes the increase of weld seam section from 2.2 mm² (plasma arc only) or 1.8 mm² (laser beam only) up to 6 mm². The depth and the width of the weld seam increase by defocusing of the laser spot. The largest weld seam sections were found for a focus position displacement Δz of 7 mm above the workpiece. Consequently, the highest degree of melting efficiency was not found for the highest focal laser beam intensity.

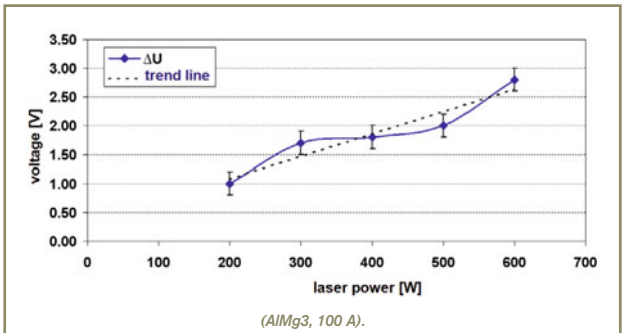

(AlMg3, 100 A).

Figure 3 – Reduction of plasma arc voltage as a function of laser beam energy

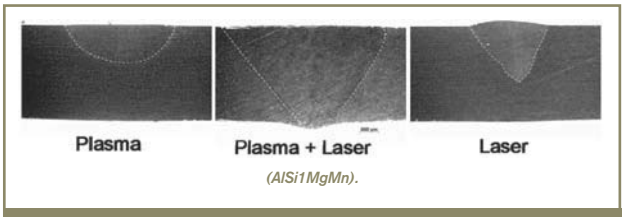

Figure 4 – Penetration profiles due to plasma arc (100 A) and laser (600 W, z = 0) and a plasma-laser process

The supporting effect on the arc attachment by a laser was however not observed for welding mild or stainless steel sheets. A possible explanation could be that the arc column and attachment is anyway in a very stable condition. The establishment of a second off axis arc attachment was consequently not observed. However the welding speed of 0.3 m/min was considerably low.

The switching on of the laser beam does not cause a decrease but an increase of the arc voltage. Measured values were in the range of up to 0.5 V for all investigated steels, Figure 5. It was furthermore observed that the arc is less stable, which can be concluded from the increased amplitudes of the voltage signal of the combined process. In contrast to aluminium the arc attachment was obviously not enhanced.

Figure 6 shows the cross-sections of a S 235 mild steel (top) and a 1.431 stainless steel (bottom) weld. It is good to see that the cross-sections of the laser-arc welds exceed the sum of the sections of the single laser and plasma arc welds. The obvious high penetration depth in stainless steel is mainly caused by keyhole effects and the low thermal conductivity of the base material.

Additionally, the influence of the process gas on the arc characteristic was investigated. The shielding gas composition was chosen in order to increase the laser beam absorption and influence the arc properties, respectively. The following gases have appreciable emission lines in the range of the laser wavelength of 1 070±5 nm [11]:

Figure 5 – Voltage characteristic of the plasma arc before and after the switching on of the laser (stainless steel)

- nitrogen (N I: 1 069 nm, 1 071 nm)
- neon (Ne I: 1 067 nm, 1 069 nm)
- carbon (C I :1 068 nm, 1 069 nm)
- silicon (Si I: 1 067, 1 069)

Gas mixtures of argon and 16 % nitrogen and CO_2 as well as 10 % neon were tested in experiments with steel. Therefore the first half of the probes was done with the plasma process only. The second half of the plates was done with the laser-plasma process. The welding experiments with these gases demonstrate results similar to the tests with argon. There were no indications of an increased arc constriction due to the switching on of the laser, in particular no changes in arc shape and size were found in the high speed video recordings. Furthermore, no decrease of arc voltage or guidance of the arc attachment was found, which is comparable to the effects on aluminium. The influence of laser absorption was not increased due to gases with absorption lines in the range of the laser wavelength.

4 Modelling the laser arc interactions

The commercial software package ANSYS CFX was used to model the plasma arc process with consideration of

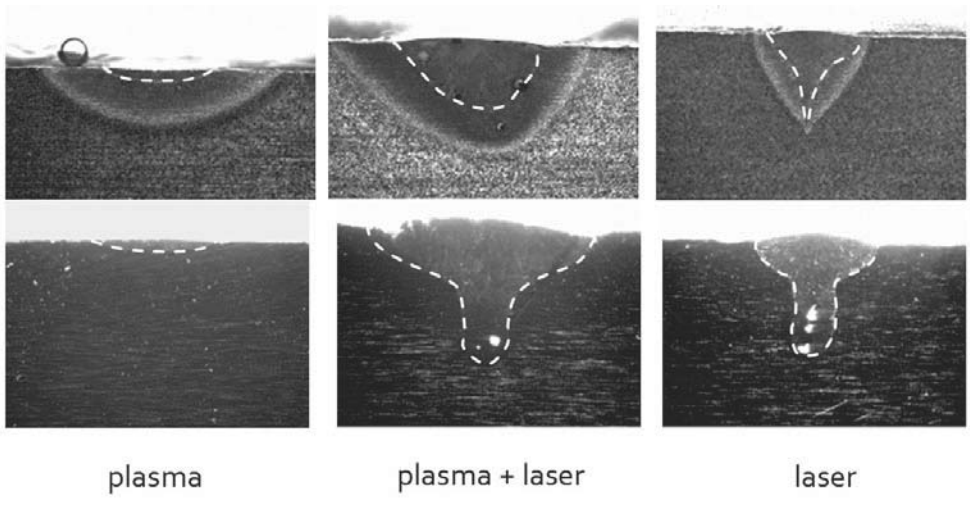

(Top: S 235 mild steel, bottom: 1.431 stainless steel).

Figure 6 – Penetration profiles due to plasma arc (100 A) and laser (600 W, z = 0) and a plasma-laser process

different kinds of interaction with a laser beam. In contrast to the experimental set-up, the model regards a concentric configuration of the arc and the laser beam. Thus the model was simplified assuming an axis symmetric steady-state approach.

The standard equations of computational fluid dynamics (conservation of mass, momentum and energy) were used. Additionally, the electromagnetic and radiative phenomena that occur in thermal plasmas were taken into account. The changes required are the addition of resistance heating and radiative loss terms to the energy equation and a magnetic pinch term (j × B) to the momentum equation; j is the current density and B is the magnetic field. Two further equations are required: an equation for current continuity

$$\nabla \cdot j = -\nabla \cdot (\sigma \nabla \varphi) = 0,$$

where

σ is the electrical conductivity and

φ is the electric potential,

and an expression for the magnetic field $B = \nabla \times A$, where the magnetic vector potential A is given by $\nabla^2 A = -\mu_0 j$, μ_0 being the permeability of free space.

The effects of the sheaths, i.e. the cathode and anode drop zones, are modelled using the sheath model of Lowke and Sansonnes [12, 13]. A detailed description of the sheath model assumptions, the mesh and the boundary conditions are given in [9, 10].

The computational domain includes a simplified shape of the torch and the workpiece and the fluid/arc region. The shielding gas fraction is defined as of pure argon at the plasma gas inlet, at the shielding gas inlet and at the ambient opening. The plasma gas inflow rate is 0.8 l/min, the shielding gas inflow rate is 12 l/min.

The plasma is assumed to be in local thermodynamic equilibrium (LTE), as it is usual for models of welding arcs. The properties were calculated for a chemical equilibrium composition. The thermodynamic properties of the species were calculated previously by Murphy [14] for a temperature range of 300-30 000 K [15]. Radiation is considered using the net emission coefficient (NEC) model. The coefficients are given as a function of plasma temperature and pressure. The 1 mm sphere iron vapour data of Menart and Malik [16], as well as the 1 mm sphere data of argon [17], were taken into account, since these data represent approximately the size of the high-temperature region. For mixtures of argon and iron vapour, the net emission coefficient is calculated as a mole-fraction weighted average as recommended by Cressault *et al.* [18].

The laser beam intensity was modelled by the given function of a beam radius r(z) using the following beam propagation equation

$$r(z) = r_0 \cdot \sqrt{1 + \left(\frac{z}{z_r}\right)^2} \qquad (1)$$

where

z is the coordinate in beam propagation direction and

z_r is the Rayleigh length given by

$$z_r = \frac{\pi \cdot r_0^2}{M^2 \cdot \lambda} \qquad (2)$$

The beam geometry according to relation (1) was determined for the laser wavelength λ of 1 070 nm, the beam quality number M^2 of 1.15 and the focus radius r_0 of 20 µm. The local intensity $I(r,z)$ of the laser beam was described by a normal distribution:

$$I(r,z) = \frac{2P_L}{\pi \cdot (r(z))^2} \cdot \exp\left(-\frac{2 \cdot r_0^2}{(r(z))^2}\right) \qquad (3)$$

The focus position of 1 mm above the workpiece was defined. Figure 7 shows on the left hand side the laser beam intensity and the vector plot of the plasma flow, on the right hand side the temperature of a 80 A arc. The results are based on the assumption that 10 % of the laser beam is absorbed in the arc. The heating effect of the laser radiation in interaction with the arc plasma is good to see by the modified shape of the isotherm near the arc and laser beam axis.

Using the developed model three possible laser effects and their influence on the arc were investigated:

(I) absorption of the laser energy in the arc column and plasma heating,
(II) induction of metal vapours on the surface or in the keyhole and its influence on the electric conductivity of the arc plasma,
(III) absorption of the laser on the surface of the workpiece inducing a hot spot.

The laser beam energy absorption in the arc column was defined according to the local laser beam intensities,

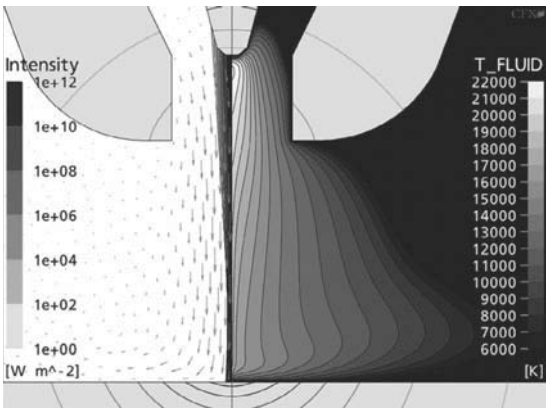

Figure 7 – Numerical simulation of the plasma laser process with an assumed overall laser beam absorption in the plasma column of 10 % (left: defined laser intensity, right: predicted plasma temperature distribution)

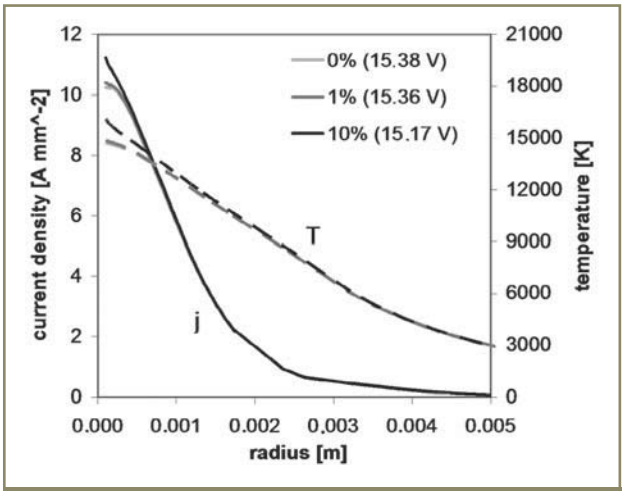

Figure 8 – Numerical predictions concerning the influence of the laser absorption in the arc plasma (relating to 600 W laser beam energy) on the plasma temperature and the electric current density 0.2 mm above the workpiece (80 A)

(1-3). Running a parameter analysis, 0, 1 and 10 % of the laser beam energy of 600 W were assumed to be absorbed by the arc plasma. The effect of the laser energy input into the arc column is shown in Figure 8, in particular the plasma temperature and the electric current density in a plane 0.2 mm above the workpiece.

The numerical results predict an increase of arc temperature and low raise of current density but only for absorption of 10 % or 60 W. However, both appear only in the very small region of the laser beam or at an arc radius of 0.3-0.5 mm. Thus, the effects of the direct absorption of laser energy on the arc properties are quite week, regarding that an assumption of 10 % arc absorption is probably disproportionately high in particular for near-infrared wavelengths. It seems that the increase of electric conductivity is too low, which is also reasoned in the high plasma temperatures and the thereby caused relatively high electric conductivity.

Modelling the influence of metal vapour, a part of the surface of the workpiece was defined as an inlet. The boundary has a radius of 40 µm, which corresponds approximately with the radius of the laser beam and the keyhole. A flow of iron vapour was defined with a temperature of 3 023 K and with a variable inlet velocity of 0 m/s (diffusion only), 100 m/s and 600 m/s. These values are in accordance with experimentally determined metal vapour velocities above the laser-induced keyhole during deep penetration laser beam welding in the range of 100-800 m/s [19].

The calculation of the metal vapour concentration within the arc plasma region considers convective and diffusive transport phenomena as well. The diffusive transfer is modelled by use of a binary diffusion model taking into account the diffusion of metal vapour relative to argon. It is based on a conservation equation for iron vapour mass fraction y_{Fe} [9, 15]:

$$\frac{\partial(\rho\, y_{Fe})}{\partial t} + \text{div}\,(\rho\vec{u}\, y_{Fe} + \vec{J}_{Fe}) = 0 \qquad (4)$$

with the iron vapour diffusion mass flux J_{Fe}:

$$\vec{J}_{Fe} = \frac{n^2}{\rho}\bar{m}_{Fe}\bar{m}_{Ar}(D^{x}_{FeAr}\ \text{grad}\ x_{Ar} + D^{p}_{FeAr}\ \text{grad ln}\ p_{tot} + D^{E}_{FeAr}\vec{E}) - D^{T}_{FeAr}\ \text{grad ln}\ T \qquad (5)$$

where the terms describe diffusion due to the gradient in the mass fraction of argon, the gradient in the total pressure, the electric field of the arc and the temperature gradient, respectively. The m_k are the average molar masses of the heavy species and the D'_{FeAr} are combined diffusion coefficients which are shown in [15].

The model predicts a decrease of the arc voltage only for an inlet velocity of 100 m/s. In contrast the arc voltage increases referencing a high vapour inlet velocity of 600 m/s. Figure 9 a) shows the predicted metal vapour concentration and the arc plasma temperature.

It is obvious that low vapour velocities in the keyhole cause a thin layer of iron vapour above the surface of the workpiece. This layer corresponds with a region of low plasma temperatures. The existence of metal vapour causes a substantial increase of the electric conductivity. The left top picture of Figure 9 shows furthermore a vapour concentration on the fringe region of the arc. The iron fraction is only visible due to its logarithmical scaling. However, it results from the diffusion effects which enable a vapour flux directed against the flow. The effects of demixing cause an accumulation of iron vapour near the 5 000 K isotherms as it was already predicted for gas metal arc welding [15].

The right top of Figure 9 shows the predicted vapour concentration and the plasma temperature for a vapour keyhole velocity of 600 m/s. The metal vapour concentration plot shows on one hand side the iron vapour plasma torch above the workpiece and, on the other hand side, significant iron accumulation on the fringes of the arc. They both affect the plasma temperature of the arc column. The iron vapour plasma jet from the keyhole causes a local decrease of plasma temperature due to the considerably increased radiation emission. As suggested by Menart [16] the radiation emission intensity of iron vapour is always higher at least in order of two magnitudes. Thus the local energy requirement ensuring an electric conductivity increase and a central minimum in the radial temperature and current density contribution is caused.

The second iron vapour accumulation in the fringes region of the arc constricts the arc. Due to the metal vapour an increase of radiation emission and electric conductivity is caused. Both effects cool probably down the fringes of the arc. However, the axial temperature distribution is not significantly affected except for the region of the plasma arc above the keyhole. High speed video records using interference narrow band pass filter centred at 530 nm

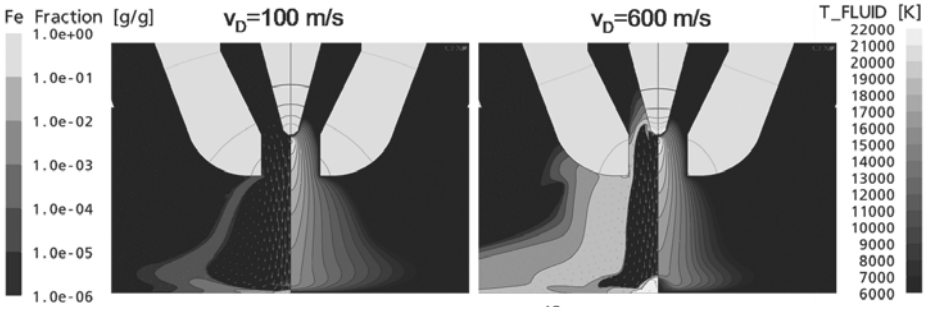

a) Numerical predictions concerning the influence of the metal vapour flow velocity v_D at the top of the keyhole on the metal vapour concentration and the plasma temperature distribution

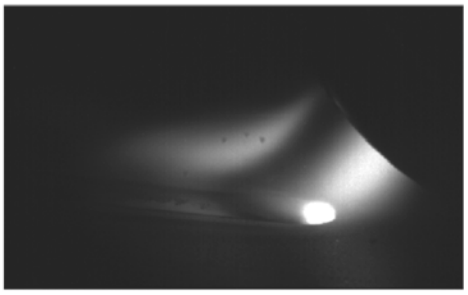

b) Demixing effects of metal vapour during plasma laser welding of steel (high speed video using a 530 nm filter)

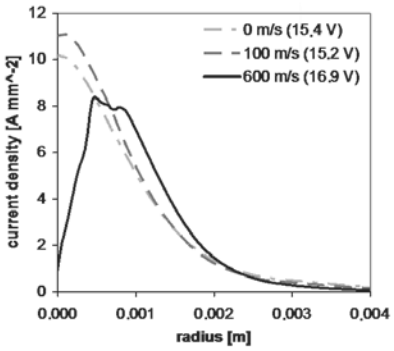

c) Num. predicted electric current density 0.2 mm above the workpiece, depending on vapour keyhole velocity

Figure 9

show the iron vapour plasma region above the workpiece and also the iron vapour accumulation on the fringes of the arc.

The diagram in Figure 9 c) shows the numerically predicted radial distributions of the electric current density in a plane 0.2 mm above the workpiece. The presence of metal vapour influences the current density at the workpiece. Low keyhole exhaust velocities of metal vapour cause a moderate increase of about 10 %. High metal vapour velocities at the keyhole induce a central minimum in current density distribution. It is obvious that this central minimum of current density can cause instabilities of the arc attachment at the workpiece. Thus, the numerical results provide some reasons of the experimentally observed arc voltage characteristics for welding steel specimen after the laser is switched on, see Figure 5. The predictions state reasons for an increase of the voltage drop and the enlarged ripple as well.

The influence of the laser absorption on the surface of the workpiece was investigated, defining the thermo physical properties of aluminium. The modelled workpiece is 5 mm-thick and the lower boundary was assumed to be water-cooled. Thus, a fixed temperature value of 300 K was defined. Furthermore the laser caustic definitions were changed, the model simulates on a focus point displacement z_L of 7 mm above the workpiece.

Figure 10 shows the influence of the absorbed laser energy at the workpiece on the radial distribution of the current density on the workpiece surface.

The predictions demonstrate that the increased surface temperatures influence the current density at the workpiece surface and the arc voltage, but the effects on the arc plasma temperature and current density are very low.

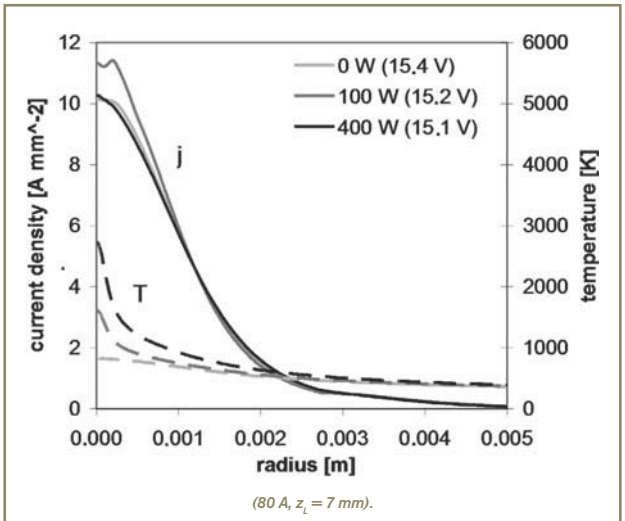

(80 A, z_L = 7 mm).

Figure 10 – Current density 0.05 mm above an Al-workpiece and surface temperature as a function of the absorbed laser energy

In contrast to low current TIG arcs the temperature of the 80 A plasma arc column is mainly determined by the nozzle type and the plasma flow [9, 10]. Thus the workpiece temperature distribution influences probably only the arc attachment. Admittedly the model predicts a small influence on current density but only for a high beam absorption. The model predictions indicate that the significant reduction of arc voltage in case of welding aluminium is not explainable without the local removal of oxide layers and metal vaporization. However, it is to mention that the sheath model used is based on some assumption and important simplifications. Thus the given predictions about the arc constriction above the workpiece need some more clarification.

5 Summary and conclusions

The interaction between a low energy fibre laser and plasma arc were investigated by experimental trials and numerical simulation as well. The experimental analysis revealed the following insights:

1. In case of welding aluminium, the laser stabilizes the arc attachment which can also be moved (guided) several millimetres apart from the axis of the arc. Due to the switching on of the laser the arc voltage and its temporal variation are decreased.
2. In case of welding ferrous alloys, the arc already establishes a stabilized attachment for welding speeds below 2 m/min without laser. It is consequently not possible to move this attachment away. Due to the switching on of the laser the arc voltage and its oscillation with time are increased. It seems that the arc is less stable.
3. The cross-sectional area of the laser-arc process is much greater than the addition of the seam areas of both single processes. This behaviour was found for aluminium, mild and stainless steels as well.
4. The largest weld seam sections were found for a defocused laser with a focus spot displacement of 7 mm (aluminium), which is equal to a laser spot diameter of 0.28 mm.
5. The gases neon and nitrogen have emission lines in the range of the laser wavelength which could increase the absorption of laser power in the arc and therefore focus the arc column. However additions in argon do not increase the effects on arc voltage (aluminium) and arc stabilization and moving the attachment (steel).

A numerical MHD model of a steady state axis symmetrical transferred plasma arc and a concentric laser beam was used for finding physical explanations of the experimental results. The numerical analyses indicate:

1. A laser arc interaction due to laser beam absorption in plasma of 6 000 K and more is implausible especially for an infrared laser wavelength of 1 070 nm.
2. The influence of laser-induced vaporization is to be discussed because of the vaporization rates or keyhole velocities.
3. Low vaporization rates and keyhole exhaust velocities affect the thermo physical plasma properties of the plasma only within a small region above the workpiece. The increased electric conductivity of plasma decreases the arc voltage and stabilizes the arc attachment.
4. High vaporization rates and keyhole exhaust velocities cause a metal vapour plume above the keyhole where the strong radiation emission of metal vapour causes a local decrease of plasma temperature and electric conductivity. Thus the main current transfer occurs off-axis. The arc voltage is increased and also instabilities can be caused.
5. The model predicts a small increase of current density due to laser absorption at the workpiece surface and locally increased temperatures. However the limitations in the validity of the model predictions, especially due to the sheath model simplifications, are mentioned.

In summary the transferred plasma arc behaviour is already almost stable on steel without a laser enhancement. An improvement of the arc attachment and its guidance by a laser spot were observed for:

– workpieces with a high thermal conductivity,
– high processing speeds,
– low welding currents or plasma flow rates,
– large angle between the plasma torch and the workpiece.

Thus, performance improvements of the combined process are mainly expected in case of high-speed welding or brazing and for micro plasma applications. The requirements for the laser beam source are probably low since the best results were observed using a comparatively wide laser beam.

Acknowledgements

This work was supported by DFG (FK: FU 307/4-1 and FK: BE 1875/19-1), which is gratefully acknowledged. Many thanks to Dr. D. Uhrlandt of Leibniz-Institut für Plasmaforschung und Technologie, Germany, for discussing these results. We acknowledge the contributions of A.B. Murphy from CSIRO, Australia.

References

[1] Seyffarth P. and Krivtsun I.V.: Laser-arc processes and their applications in welding and material treatment, London, Taylor and Francis, 2002.

[2] Steen W.M.: Arc-augmented laser processing of materials, Journal of Applied Physics, 1980, vol. 51, no. 11, pp. 5636–5641.

[3] Cui H.: Untersuchung der Wechselwirkungen zwischen Schweißlichtbogen und fokussiertem Laserstrahl und der Anwendungsmöglichkeiten kombinierter Laser-

Lichtbogentechnik – Investigation in interactions between a welding arc and a focused laser beam and the possible applications of combined laser arc techniques, PhD Thesis TU Braunschweig, 1991 (in German).

[4] Cui H., Decker I., Pursch H., Ruge J., Wendelstorf J. and Wohlfahrt H.: Laserinduziertes Fokussieren des WIG-Lichtbogens, Laser induced focusing of a TIG arc, DVS-Bericht, Bd. 146, Düsseldorf: DVS-Verlag GmbH, 1992 (in German).

[5] Decker I., Wendelstorf J. and Wohlfahrt H.: Laserstrahl-WIG-Schweißen von Aluminiumlegierungen, Laser-TIG-welding of aluminium alloys DVS-Bericht, Bd. 170, Düsseldorf: DVS-Verlag, pp. 206-208, 1995 (in German).

[6] Albright C.E., Eastman J. and Lempert W.: Low-power lasers: Assist arc welding, Welding Journal, 2001, vol. 80, no. 4, pp. 55-58.

[7] Hermsdorf J.: Lasergeführtes MSG-Schweißen – Flexibles, lasergeführtes Lichtbogenschweißen für das prozesssichere Fügen von Stählen, höher- und hochfesten Stählen und Leichtmetallen, Laser-guided GMAW for joining of steels, high-strength steel and light metals, Photonik 4, 2006 (in German).

[8] Kling R., Otte F., Stahlhut Ch. and Hermsdorf J.: Minimale Laserleistung mit Lasern angepasster Strahleigenschaften für das Laser/MSG-Hybrid-Schweißen in Fertigungssystemen für die Fahrzeugfertigung, Minimal laser power due to laser beams with adapted beam properties for welding in automotive production, DVS-Bericht, Bd. 244, Düsseldorf: DVS-Verlag, 2006, pp. 409-412 (in German).

[9] Schnick M.: Numerische und experimentelle Beschreibung des Plasmalichtbogenschweißens, Numerical and experimental investigation of plasma arc welding, PhD-Thesis, TU Dresden, 2011 (in German).

[10] Schnick M., Fuessel U. and Spille-Kohoff A.: Numerical investigations of the influence of design parameters, gas composition and electric current in plasma arc welding (PAW), Doc. IIW-1997, Welding in the World, 2010, vol. 54, no. 3/4, pp. R87-R96.

[11] http://physics.nist.gov/PhysRefData/Handbook/index.html: Homepage: National Institute of Standards and Technology, Gaithersburg, 2009.

[12] Lowke J.J., Tanaka M.: 'LTE-diffusion approximation' for arc calculations, Journal of Physics D: Applied Physics, 2006, vol. 39, no. 16, pp. 3634-3643.

[13] Sansonnens L., Haidar J. and Lowke J.J.: Predictions of properties of free burning arcs including effects of ambipolar diffusion, Journal of Physics D: Applied Physics, 2000, vol. 33, no. 2, pp. 148-157.

[14] Murphy A.B.: Thermal plasmas in gas mixtures (Topical Review), Journal of Physics D: Applied Physics, 2001, vol. 34, no. 20, pp. R151-R173.

[15] Schnick M., Fuessel U., Hertel M., Haessler M., Spille-Kohoff A. and Murphy A.B.: Modelling of gas-metal arc welding taking into account metal vapour, Journal of Physics D: Applied Physics, 2010, vol. 43, no. 43, 434008.

[16] Menart J. and Malik S.: Net emission coefficients for argon-iron thermal plasmas, Journal of Physics D: Applied Physics, 2002, vol. 35, no. 9, pp. 867-874.

[17] Evans D.L. and Tankin R.S.: Measurement of emission and absorption of radiation by an argon plasma, Physics of Fluids, 1967, vol. 10, pp. 1137-1144.

[18] Cressault Y., Teulet P. and Gleizes A.: Thermal plasma properties in gas or gas-vapour mixtures Proceedings of the 17th International Conference on Gas Discharges and their Applications, Cardiff, 7-12 September 2008, ed. J E Jones (Cardiff: GD2008 Local Organizing Committee), 2008, pp. 149-52.

[19] Beyer E.: Schweißen mit Laser – Welding with laser beam, Berlin – Heidelberg – New York: Springer-Verlag, 1995 (in German).

About the authors

Dr.-Ing. Michael SCHNICK (michael.schnick@tu-dresden.de), Dipl.-Ing. Sascha ROSE (sascha.rose@tu-dresden.de), Prof. Dr.-Ing. habil. Uwe FÜSSEL (uwe.fuessel@tu-dresden.de), Dr.-Ing. Achim. MAHRLE (achim.mahrle@iws.fraunhofer.de), Dipl. Math. Cornelius DEMUTH (cornelius.demuth@iws.fraunhofer.de) and Prof. Dr.-Ing. Habil. Eckhardt BEYER (eckhard.beyer@tu-dresden.de) are all with Institute of Surface and Manufacturing Technology, Dresden University of Technology, Dresden (Germany).